

GODDARD GRANT

IN-47-CR

111336  
35 p

CLOUD COVER DETERMINATION IN POLAR REGIONS  
FROM SATELLITE IMAGERY

R.G. Barry, J.A. Maslanik, and J.R. Key

Cooperative Institute for Research in Environmental Sciences  
and  
Department of Geography  
University of Colorado, Boulder

Semi-Annual Report  
to  
NASA Climate Program

Grant: NAG-5-898

29 December 1987

(NASA-CR-181544) CLOUD COVER DETERMINATION  
IN POLAR REGIONS FROM SATELLITE IMAGERY  
Semiannual Report (Colorado Univ.) 35 p

CSCL 04B

N88-12908

Unclas  
G3/47 0111336

## 1. INTRODUCTION

The goal of this research is to improve on our understanding of the spatial, textural, and multispectral characteristics of cloud cover in the polar regions in relation to atmospheric and surface conditions. This objective is directly applicable to improving cloud classification in the Arctic and Antarctic using manual and digital methods.

Techniques for detecting cloud cover from visible and infrared satellite-measured radiances include threshold methods, statistical methods, and radiative transfer methods. Rossow et al. (1985, p. 885) compared six ISCCP (International Satellite Cloud Climatology Project) algorithms and found that some of the largest disagreements occur over cold snow-covered land areas. These methods often fail in the polar regions due to:

1. low radiances, in general;
2. low radiance contrasts between cloudy and clear scenes;
3. complex surface property variations caused by changes in snow and sea ice, and
4. non-monotonic relations between radiances and cloud properties.

Sea ice can be as reflective clouds in the short-wavelength portion of the optical spectrum (e.g., Raschke, 1987), and the thermal structure of the troposphere is characterized by frequent isothermal and inversion layers. In addition, the polar darkness during winter makes that data from the visible portion of the spectrum largely unavailable. Because polar surfaces and troposphere are characterized by extremely low surface temperatures and solar illuminations, satellite radiometers operate near one limit of their performance range. Low radiances magnify the effects of instrument noise, calibration uncertainties and digitization on radiance accuracy. Weak polar temperature lapse rates reduce the infrared radiance contrast

between cloudy and clear scenes and the inversions may even reverse them. The difference for IR split window channels (AVHRR channels 4 and 5) is often reversed in winter due to boundary layer inversions and water cloud. Also, there is a maximum concentration of aerosols in the Arctic spring when the solar zenith angle is large. Additional research is required to further quantify the above effects as well as the general characteristics of clouds in the Arctic and Antarctic, and to determine the degree to which spectral and textural properties can be used to map cloud cover in the Arctic and Antarctic.

## 2. OBJECTIVES

Analysis of clouds in polar regions can be performed manually, digitally, or through a combination of manual and computer-aided decisions. Regardless of which interpretation method is used, all underlying classification steps must be based on a sound knowledge of the spectral, spatial, and textural characteristics of clouds in the Arctic and Antarctic, as well as the probabilistic distribution of these characteristics for a given cloud type under a given set of meteorological conditions. Although a variety of sophisticated digital techniques can be applied to cloud analysis, an understanding of the limits, and therefore the capabilities, of these techniques for polar cloud mapping requires more basic information than is currently available in the literature.

Manual interpretation of satellite imagery for the polar region is largely successful because the interpreter is combining spectral, textural and contextual knowledge in the process (e.g. Robinson et al., 1986; Barry et al., 1987). Unfortunately, manual interpretation is time consuming and largely subjective (McGuffie et al., 1987). A key goal of this study is to determine which spectral and textural features are most useful in the parameterization of clouds from satellite data in the polar

region, and how these features may be combined with various classification algorithms for cloud detection and analysis.

Cloud classification over polar regions is complicated by a wide range of potential surface conditions caused by changes in snow/ice albedo and sea ice concentration. Typical albedos for cloud types may vary according to underlying surface conditions that change over time. Another goal of this research is to investigate total reflectivity over different surface types, and to determine whether surface information provided by passive microwave data can be used to at least partially constrain the "surface condition" variable within the overall equation for cloud classification.

Specifically, the objectives are to

1. examine the textural and spectral characteristics of polar "surfaces" with emphasis on clouds;
2. reduce the dimensionality of the spectral and textural feature sets to those features which yield the greatest discriminatory capability, and create a catalog of these features, or "object" definitions;
3. examine the usefulness of combining visible, infrared, and microwave data for analysis of polar surfaces and cloud types;
4. apply the spatial coherence, dynamic threshold, and portions of the ISCCP algorithms and determine what modifications are necessary for use with polar data;
5. apply fuzzy and hard cluster algorithms to the problem of cloud and surface type clustering;
6. extract a set of cloud properties from each of the above methods, and compare the algorithms in terms of accuracy, usefulness, and overall "power".

As an outcome of this work, we seek develop and demonstrate a methodology that can produce a uniform, map-projection based data set combining imagery from different satellites and sensors. Such a data set can be easily combined with other forms of information, and can serve as a standard set of imagery that can be used for algorithm comparisons.

### 3. METHODOLOGY

Since the objectives of this study are to produce data and information (e.g. imagery sets and spectral/textural properties) that can be used by other researchers, a methodology has been employed that attempts to reduce many of the unknowns that can make the results of remote-sensing studies difficult to interpret and apply. These unknowns can include questions concerning data calibration, resampling, spatial and radiometric resolution, and corrections for systematic errors due to bidirectional reflectance and solar zenith angle. Differences in how these and other processing steps are handled often make it difficult to extrapolate the results of individual studies to other research and to compare the performance of different classification schemes. The methodology defined for this project has been developed to assure that basic information on the spectral and textural characteristics of polar clouds has been gleaned from a well-documented set of data, and that this information is presented in a form directly applicable to other studies. Portions of this procedure have been defined and applied previously to the study of polar clouds by Ebert (1987). The methods to be used include: (1) generation of a set of imagery consisting of reflectance, radiance, and temperature data calibrated according to sensor parameters, (2) geometric rectification of this imagery to a map projection suitable for digital analysis and combination with imagery and data from other sources such as pressure charts, buoy information, and passive microwave-derived ice concentrations, (3) investigation of the effects of systematic errors such as viewing angle and anisotropic reflectance to determine if systematic corrections are required, (4) manual interpretation of selected images to provide a baseline classification of clouds and surfaces, (5) determination of the separability of cloud classes from surfaces by statistically summarizing the spectral and temporal properties

of different cloud types over a variety of surface conditions, (6) investigation of the utility of identified characteristics for multispectral/textural classification of polar clouds, and (7) comparison of interpreted cloud cover to modelled clouds. The following sections describe the current status of these tasks.

#### 4. DATA

##### *Optical-Wavelength Imagery*

The primary source used in this study for digital imagery in the optical wavelengths (visible through thermal wavelengths) is the test data set of Advanced Very High Resolution Radiometer (AVHRR) imagery supplied as part of the International Satellite Cloud Climatology Project (ISCCP) algorithm validation program for polar regions. This set of computer-compatible tapes includes AVHRR imagery in orbital format for 5 days in July, 1984 and 5 days in January, 1984 covering portions of the Arctic and Antarctic during local winter and summer. The AVHRR data used are derived from standard Polar Orbiter Level 1b archive maintained by NOAA, and consist of partial orbits of Global Area Coverage (GAC) imagery. Each scan line contains 409 pixels, with one solar zenith angle and ground location value provided for every eight pixels. Five channels are available as follows:

Channel 1:	580 - 680 nm	(visible)
Channel 2:	725 - 1000	(visible, near infrared)
Channel 3:	3550 - 3930	(reflected/thermal IR)
Channel 4:	10300 - 11300	(thermal IR)
Channel 5:	11500 - 12500	(thermal IR)

##### *Calibration and Registration*

The following calibration and registration steps were performed to produce a standardized set of digital imagery suitable for algorithm testing and combination with other types of information. The methods applied are typical of those used for geographic information systems analysis with high-resolution data such as Landsat imagery, and are well-suited for extracting

information from multiple "layers" of data. The techniques have been adapted to accomodate the special needs of polar studies using relatively low resolution data.

First-order calibration of the AVHRR GAC data was performed using the calibration coefficients contained in the image files, and the methods described in the NOAA Polar Orbiter Users Guide (NOAA, 1984) and in Lauritsen, et al. (1979). The data values recorded in the Channels 1-5 were converted to approximate spectral albedo in percent for channels 1 and 2, and radiance in milliwatts/m<sup>2</sup>-steradians-cm<sup>-1</sup> for channels 3-5. These conversions were performed as a linear function, with slope and intercepts provided by the calibration coefficients contained in the data. The thermal radiances were also converted to approximate physical temperature in Kelvins, or brightness temperature, using an approximation of the inverse of the Planck function (NOAA, 1984). The percent albedo values produced for Channels 1 and 2 by this method are approximations of system albedo. Care is required when comparing these values to broad-band system albedos sensed over a wider spectral range.

Comparison of different images and precise calculation of surface temperatures or albedos normally requires corrections for atmospheric effects. With the exception of the solar zenith angle corrections described below, no adjustment for atmospheric effects were made. The typically low water vapor content in polar atmospheres, as well as the low physical temperature of the atmosphere, reduces most atmospheric effects to a point where they may be neglected for the type of analysis performed here. This assumption will be tested by comparing passive microwave-derived surface temperatures with temperatures calculated from AVHRR data. The effects of atmospheric haze have recently been modelled for AVHRR wavelengths (Gerstl and Simmer, 1985), and will be included in future work studying the radiative transfer properties of the polar atmosphere.

To account in part for the significant effects of solar zenith angle differences along the wide swath of AVHRR, each

Channel 1 and Channel 2 pixel value was normalized by dividing the pixel value by the cosine of the solar zenith angle for that pixel as provided in the GAC data records. Since one zenith angle is provided per 8 data pixels, the intermediate zenith angles were linearly interpreted to yield an approximate angle for each pixel. The calibration and normalization steps used do not take into account bi-directional reflectance and emittance differences. Sets of data with no zenith angle corrections have also been maintained and used to provide statistics representative of imagery without adjustments for solar zenith angle.

A final step in the AVHRR data correction involved extracting the reflected-energy component from the emitted component in Channel 3. At 3.7 micrometers, this channel records both reflected and emitted energy; the simple conversion to physical temperature used here does not separate the two contributions. Calculation of the reflected component and thermal component of Channel 3 was performed by subtracting the brightness temperature calculated for Channel 4 from that calculated for Channel 3. Channel 3 reflected radiance was then derived by passing this residual through the inverse of the Planck function relationship used for the radiance-to-temperature conversion.

#### *PASSIVE MICROWAVE DATA*

In order to provide concurrent information on surface conditions, passive microwave data in digital form were acquired and processed. The ability of passive microwave sensors to collect data independent of solar illumination and to map surface conditions through cloud cover makes SMMR particularly useful for polar studies.

The passive microwave data used in this study were acquired on January 6 and July 2, 1984 by the Scanning Multichannel Microwave Radiometer (SMMR) carried onboard Nimbus 7. The SMMR imagery used consist of data converted from NASA CELL-ALL format

to a polar stereographic projection. The 18 and 37 GHz data are mapped to grid cells with a dimension of 25x25 km at 70 degrees latitude. The 18 GHz are interpolated to accomodate the 25 km resolution grid. During the gridding process, no distinction is made between day, night, and twilight orbits, and data from overlapping orbits are averaged to yield a daily value. The data stored in these grids are recorded as brightness temperature in kelvins. Sea ice concentration and fraction of old ice were calculated from the SMMR data using the NASA Team Algorithm (Cavalieri, et al., 1984). This algorithm is based on the normalized difference between vertically- and horizontally-polarized emissivity at 18 GHz and vertically-polarized emissivity differences at 37 GHz and 18 GHz between ice, water, and ice type.

#### *Preprocessing*

Merging of the AVHRR GAC imagery and the SMMR passive microwave data into a form suitable for detailed analysis required selection of a common grid size that offers a compromise between resolution and data volume. A polar stereographic projection yielding equal-area pixels true at 70 degrees was selected as the desired map base, with a 5 km grid cell (pixel) size. This pixel size represents a slight degradation of the AVHRR GAC resolution, but has the advantage, in terms of data processing, of being an even multiple of the SMMR 25 x 25 km cells. The SMMR data were converted to 5 km cell sizes by simple duplication of pixels, thereby avoiding any artificial "improvement" in the SMMR resolution.

Re-mapping of the AVHRR data to the polar projection was performed using the ground locations in latitude and longitude provided in the GAC records for every eighth pixel. Latitude and longitude coordinates for the intermediate pixels were linearly interpolated from each eighth-pixel location. Each pixel location was then transformed from latitude/longitude to polar grid coordinates using standard map projection algorithms.

Unfilled grid cells were interpolated by an average of non-zero neighbors. At the edges of the orbit swath, the reduction in true ground resolution due to the earth's curvature is reflected by pixel duplication that yields larger "effective" pixels, although the grid cell size remains constant across the image.

In order to maintain as much radiometric resolution in the data as possible, the AVHRR and SMMR imagery were typically stored and processed in 16-bit form. For display purposes, the data were mapped to 8-bit data values to accommodate the image analysis system used. Since one of the ultimate objectives of this project is to investigate viewing angle dependencies on observed reflectivity and temperature, no adjustments were made to compensate for these effects.

#### *OTHER SURFACE AND ATMOSPHERIC DATA*

Additional information on surface and atmospheric conditions have been provided by NOAA/Navy ice charts, Defense Meteorological Satellite Program imagery, and gridded surface/atmospheric pressure and temperature data acquired by the Arctic Buoy program and the European Center for Mid-range Weather Forecasting.

#### 4. ANALYSIS TO DATE

At this stage in the project, 11 AVHRR images for the Arctic and 2 AVHRR images covering portions of the Antarctic have been extracted, calibrated, and registered using the above methods. Both summer and winter data have been processed. An additional 4 scenes for the Arctic have been extracted and calibrated, but have not yet been mapped to the polar stereographic projection used. The bulk of the analysis described in later sections has been applied to day and night scenes (4 day and 2 night scenes) for the regions shown in Figure 1. Each of these 6 scenes has been digitally merged with SMMR data to produce a combined data set covering portions of the optical and microwave spectrum, with

additional features such as sea ice concentration included in the merged data set.

Analysis to date has taken the form of manual interpretation, graphical analysis, and statistical analysis. Several images were manually interpreted to provide a cloud classification that can serve as a basis of comparison with digital techniques. The manually-interpreted cloud classes are also used to provide homogenous regions, or training areas, for which multispectral and textural statistics can be calculated. In addition, the manual analysis has been used to define the spectral, spatial, and textural characteristics that human interpreters use to discriminate between different cloud and surface, and between different types of clouds.

#### *Basic Statistics for Cloud and Surface Conditions*

Spectral, textural, and contextual feature types have been examined to some extent as part of this project, and will be defined further as work progresses.

Statistics describing reflectance, thermal-wavelength temperature, microwave brightness temperature, and texture for a variety of cloud and ice conditions were extracted from the merged AVHRR/SMMR data sets. Cloud classes were manually interpreted using an interactive image analysis system. The merged imagery was displayed using several combinations of spectral channels to produce a range of false-color composites. Interpretation of cloud cover and ice conditions was greatly aided by this machine-assisted approach, which allows the interpreter to switch in real-time between combinations of co-registered AVHRR and SMMR imagery. For example, in clear-sky conditions, locations of ice margins were mapped using AVHRR imagery, while the SMMR data were used to map ice conditions beneath cloud cover.

Analysis was performed using a DIPIX ARIES IV image analysis system, the SAS statistics package, and custom software.

### A. Viewing Angle Effects

The bi-directional reflectance of snow cover is not uniform (Steffen, 1987), and the measured reflectivity and emissivity of snow cover varies with satellite viewing angle. In order to investigate these effects and possible angle dependencies for snow, ice, and cloud cover in the AVHRR imagery, reflectivity, thermal radiance, and thermal temperature were plotted versus viewing angle (0 to  $\pm 55.4$  degrees) for several cloud and sea ice classes defined in a single images. Examples for imagery without solar zenith angle corrections are shown in Figure 2. The large scatter apparent in many of these plots makes precise interpretation difficult; however, a trend of increasing thermal temperature at increasing angles of forward scatter is apparent. Further work is underway to determine whether this pattern appears in other images oriented differently relative to latitude since, in the image plotted, the AVHRR scanner is looking approximately northwards at  $-50$  degrees, and southward at  $50$  degrees. The results to date are limited by the relatively small number of polygons, or "samples", available per class, and will become more significant as additional AVHRR images are processed. Since corrections for viewing angle differences assume knowledge of surface or atmospheric condition, it is questionable whether such corrections should be applied to raw data prior to classifying mixed surface and cloud areas. Better results might be achieved by stratifying the data into broad approximate classes, and then applying the appropriate corrections separately for the different major classes of cloud, snow and ice, and open water.

### B. Multispectral Characteristics

Raw spectral features, ratios, sums, and differences have all been utilized in classification studies of satellite data. Here,

spectral features examined for each cell (an array of contiguous pixels; discussed below) include the following:

1. mean
2. standard deviation
3. maximum
4. minimum
5. the ratio of maximum to minimum
6. range
7. ratios between albedos of channels 2 and 1, and 3 and 1 of the AVHRR data
8. difference between channels 4-5 (BTD), 4-3, and 2-1

Seventeen surface and cloud classes are of interest:

1. Land (clear sky)
2. Water (clear sky)
3. Sea ice (clear sky; various concentrations)
4. Snow (clear sky; various ages)
5. Low cloud
6. Middle cloud
7. High cloud
8. Mixed cloud
- 9-17. Low, middle, and high cloud over land, water, and ice

Not all of these classes will be included in every analysis; e.g. the manual classification was done for only classes 1-8. Where necessary, classes 9-17 are derived from classes 5-7 using digitized land boundaries and SMMR-derived sea ice concentrations. For all classes involving sea ice, ice concentrations are estimated using the SMMR data. Estimates of albedo and texture obtained from the AVHRR imagery can therefore be related accurately to ice concentrations. The SMMR-derived ice information also allows us to measure the albedo and texture of clouds above a range of ice concentrations.

The manually interpreted classes (serving as training areas) were used to define the multispectral signatures of different types of cloud, sea ice, and cloud-over-sea ice conditions. Results for several of these classes for zenith-angle corrected data, plotted by mean  $\pm$  two standard deviations, are shown in Figure 3. The overlapping distributions for many of the classes indicate the poor separability of cloud and sea ice classes using only the AVHRR visible (Ch. 1) and thermal channels (Chs. 4, 5). As expected, separability between cloud and ice is greater in Ch. 3 (reflected component only; and also somewhat greater in Ch. 2 compared to Ch. 1 due to the lower reflectivity of ice crystals at longer wavelengths. The difference may be enhanced due to the presence of liquid water in the melting ice pack. Differences in reflectivity are also apparent in Ch.3 between high cloud composed of ice crystals, and lower cloud made up of liquid water. Comparison of thermal temperature reveals the expected differences between the warm land and other classes. The mean temperature for open water in the polar oceans is shown to be about 272 K. Sea ice temperature shows very little variability, and is close to the 273 K value expected for melting sea ice.

The multispectral cluster plots (manually classified data with no zenith angle corrections) shown in Figure 4 illustrate the sources of confusion and distinction between different cloud and surface classes. Cluster diagrams using training areas (areas likely to represent more "pure" classes than those defined by the more general manual classification) yield more discrete clusters. The diagrams shown are, however, typical of the situation faced by automated classifiers, and represent the variability of cloud and surface conditions present. Some of the general confusion between classes can be resolved using the SMMR data. Figure 5 demonstrates how SMMR data combined with AVHRR imagery can be used to separate cloud over land from cloud over water due to the large difference in microwave emissivity of land and water. Similar plots demonstrate the ability of the merged AVHRR and SMMR data to distinguish between cloud over ice and

cloud over water. The examples shown are typical of the types of plots currently being generated to help define spectral characteristics.

Additional, site-specific, information on multispectral properties is provided by transect plots that present albedo, thermal temperatures, and brightness temperatures at individual pixel locations. An example of such a plot is shown in Figure 6. The plots show the correlation between albedo and ice concentration, and the radiances of clouds over different surfaces.

### C. Textural Information

The simplest textural features are first-order statistics that describe the distribution of individual pixel features such as intensity. Second order statistics summarize the probability (relative frequencies) of the intensity values of a pair of pixels. These probabilities are computed for each pair of pixels in a given positional relationship and are summarized in a co-occurrence matrix. Higher order textural statistics may also be used, however, they generally involve more computation and do not necessarily give better results.

Texture Measures. Texture measures have been calculated for a variety of data types and spectral bands. In this study, texture measures are computed for AVHRR channels 1, 3, and 5. Textural features employed follow those presented in Haralick et al. (1973), Haralick and Shanmugam (1974), Parikh (1977), Wu et al. (1985), and Ebert (1987). The texture measures computed are:

1. Standard deviation
2. Roberts gradient
3. Vector strength
4. 2-dimensional Fourier analysis

## 5. Grey level difference measures:

- a. Mean
- b. Contrast
- c. Angular second moment
- d. Entropy

The maximum harmonic amplitude and coordinates were extracted from the Fourier analysis. Each of the grey level difference measures were computed over four directions and across a variety of pixel separation distances. The maximum of the four directions with a separation distance of one are being employed in subsequent analyses.

Figure 7 shows some examples of the variability in albedo and temperature within 25 x 25 cell areas, and is typical of the types of the graphical analyses being used to define characteristic textures for polar surfaces. The sample shown in Figure 7 demonstrates similarity, and thus an inability to discriminate, between low cloud over water (relatively warm with a moderately high albedo) and sea ice undergoing surface melt (again, relatively high temperature and fairly high albedo). However, when spatial variability of albedo and temperature (rather than magnitudes alone) are considered, differences appear between sea ice and cloud. It is hoped that such analyses will produce characteristic spatial textures that can be quantified and used as addition information to discriminate clouds from ice and snow. The basic information of the separability of cloud and surface classes in the polar regions acquired using texture measures at different cell sizes will be reviewed in the next stage of this study to determine possible application as classifiers.

Cell Size. Textural features are calculated for groups of contiguous pixels called cells. Because of this grouping of pixels, image resolution is reduced and some information is lost, although textural information may be gained. The issue of cell

size is important in that too large a cell may blur the boundaries between classes, while too small a cell may not allow for adequately describing the textural and spectral features which distinguish between the classes. In addition, the larger the number of pixels in each cell, the more acceptable the dependent statistical summaries will be. A variety of cell sizes have been used in previous studies of clouds, with no particular test or justification offered to explain why a particular cell dimension was chosen. To help define an optimal, or set of optimal, cell sizes for polar cloud mapping, the effect of cell size on texture calculations and the ability to differentiate between classes was examined.

To determine an upper limit on cell size, sections of an image were displayed based on means of the cell sizes 4x4, 8x8, 12x12, and 16x16. (Since cells are square, hereafter cell sizes will be referred to by only one dimension.) Resolution with cell sizes 4 and 8 is acceptable; conversely, a cell size of 16 seems to degrade the image such that objects of interest are quite distorted. After this subjective analysis then, cell sizes greater than 16 are clearly unacceptable.

Seven of the texture measures were calculated from cell sizes of 8, 10, 12, and 16 for ten cloud and surface areas. A paired t-test was then applied to test the difference between cells sizes of 8 and 16, 8 and 12, 12 and 16, and 10 and 16. The null hypothesis was that there is no difference between the population means. Results are indicate that in three of the seven tests there appears to be a significant difference between cells of sizes 8 and 16, and in no cases can we conclude that there is a significant difference between texture measures extracted from cells of sizes 12 and 16. Other pairs show results between these two extremes.

Finally, the behaviour of these seven texture measures for cell sizes from 20 down to 2 was examined graphically. In most cases, the texture measures either remain constant or decrease linearly with decreasing cell sizes down to 6 where they become

erratic. Based on these tests a cell size of 10 was chosen and is used in subsequent analyses.

#### D. Multispectral Classification

The work described above to quantify the spectral and textural properties of polar features is directly applicable to the development and testing of multispectral and/or "multi-textural" classifiers. The following sections describe our ongoing efforts to relate these basic characteristics of polar surfaces to multispectral classification schemes.

Threshold Methods. Multispectral threshold methods vary considerably in how clear and cloudy sky radiances are determined. The spatial coherence method of Coakley and Bretherton (1982) examines the local spatial structure while the ISCCP algorithm depends more heavily on temporal variance in observed radiances. Neither method has been successfully applied to polar regions.

Spatial coherence has typically been applied to single layer cloud systems over open water in tropical regions. It was later modified by Coakley (1983) and Coakley and Baldwin (1984) for application to two-layer cloud decks. In the polar region data used here, these cases are the exception rather than the rule. Surface types are snow-covered and snow-free land, sea ice of varying concentrations and ages, and patches of open water. While one and two-layer cloud systems may be found, cloud systems are often complex. Figure 8 illustrates this type of spatial coherence diagram applied to an entire merged AVHRR/SMMR image. This diagram is based on 8x8 cells extracted from AVHRR channel 4. The characteristic arch can be seen, and the foot representing high cloud pixels is fairly distinct. However, at higher temperatures with low standard deviations, sea ice, snow, and low cloud are mixed together. The resulting range of physical temperatures yields one elongated cluster of temperatures

rather than the distinct "feet of the arch" typical of clouds over ocean at lower latitudes where the contrast between ocean and cloud temperatures are typically greater. The classes shown are the surface and cloud types which make cloud analysis in the polar regions difficult, in this case because of similar brightness temperatures. We may, however, isolate those portions of the image which contain a single surface and cloud type, then repeat the procedure. Figure 9 shows the resulting spatial coherence graphs. Distinctions between cloud and land, and between cloud and sea ice, are more distinct, although low cloud and water are still indistinguishable based on temperature. The purpose of the spatial coherence method is to aid in determining clear and cloudy sky radiances for the calculation of fractional cloud cover over a subregion. Ideally, this process will be automated, so that visual examination of the diagrams for each image or subarea is not necessary. However, multiple surface and cloud types makes this process considerably more complex.

Although the ISCCP algorithm takes a very different approach, it also fails when multiple surface types are involved. We have therefore begun to examine modifications to the spatial coherence and ISCCP algorithms for application to polar regions. The focus is on a methodology which accurately determines clear and cloudy sky radiances for multiple cloud layers and multiple surface types. Once these parameters are determined, an extended version of Coakley's (1987) dynamic threshold technique may be applied to determine cloud fraction by determining which threshold(s) maximizes the linear relationship between mean radiance of a region and cloud fraction.

**Cluster Methods.** Other work to date concerning the effectiveness of multispectral classifiers has involved application of a maximum-likelihood unsupervised clustering algorithm to subsets of the AVHRR/SMMR data. The results of several clustering runs were compared with the manual classifications to test how well the unsupervised clustering approach was able to duplicate the

detail and content of the manual analysis. Combinations of different spectral features were clustered to determine which sets of features provided the maximum amount of information, as well as which set provided adequate classification with a minimum amount of data. For all combinations, AVHRR Ch. 3 was required to discriminate cloud over ice. Inclusion of the SMMR data added additional classes distinguishing between cloud over ice and cloud over water. Qualitatively, good agreement was found between the manual classification and the limited set of clustering results to date. A quantitative comparison of classification results is planned. Misclassifications are most apparent at cloud boundaries where the cloud characteristics tend to deviate most from the average characteristics for that cloud class. This is especially apparent for thin cloud and low cloud that extends over several surface types.

Ideally, most classes defined for multispectral analysis are composed of mutually exclusive, or "hard", classes with well defined boundaries. With data types that are continuous over the observations (e.g. space) and do not exhibit clear boundaries, the hard classifications seem particularly inappropriate. Such diffuse boundaries in the real world should be similarly represented in taxonomic space. Since the above analysis indicates that cloud classifications are particularly sensitive to diffuse boundary errors, a classification method usually referred to as "fuzzy sets analysis" designed to address these types of classification errors is being tested (Ruspini, 1969; Bezdek, 1975). This method has, to our knowledge, seen only limited use for spatial data analysis, and has not hitherto been applied to the classification of remotely-sensed imagery.

Using the fuzzy sets approach, points are given membership values for each of the classes being constructed. Membership values are between zero and one and all the membership values for a given point must sum to unity. Memberships close to one signify a high degree of similarity between the sample point and a cluster while memberships close to zero imply little

similarity. In this respect, memberships are similar to probabilities. However, no assumption of distribution type is made in fuzzy c-means (FCM) clustering, and calculations of memberships are not based on probability density functions. Therefore, this methodology bears little theoretical relationship to probability-based techniques such as maximum likelihood (which assumes multi-variate normal distributions), and discriminant analysis (which is based on the general linear model), although conceptually it is perhaps most similar to the latter. Additionally, in contrast to maximum likelihood and parallelipiped classifiers which use fixed class means and variances throughout the application, the nature of the fuzzy c-means algorithm is such that cluster (class) centers are constantly changing until convergence is obtained.

A fuzzy sets algorithm capable of processing the merged AVHRR/SMMR data has been implemented and tested for a small subset (250 x 250 pixels) of imagery. The results have been compared to manual and unsupervised classifications. The area clasified contains open water, clear sky land, snow-covered land, high, middle, and low cloud over water, ice, and land. Means of 2x2 pixel cells in the three AVHRR channels 1, 3, and 5 were used in the analysis. The procedure was arbitrarily constrained to produce ten classes, ten being the number of classes of interest identified manually. Those areas which are either difficult to classify based on the given spectral information or have relatively fuzzy boundaries (due to either the nature of the object or the resolution of the data) or both, have low or intermediate membership values for one or more classes. This is particularly true in complex cloud systems where high, middle, and some low clouds are mixed. This also seems to be the case for the snow covered land of Novaya Zemlya, which receives low/intermediate membership values for a few of the classes. These are areas that - at least for this particular algorithm - need additional information to be distinguished from other classes.

The fuzzy sets classifier appears clearly capable of detecting those areas that have a high likelihood of misclassifications using decision-rule classifiers such as the threshold and clustering methods typically used for cloud classification. Further work is underway to interpret the fuzzy sets results and to apply the fuzzy sets classifier to different sets of imagery.

## 5. SUMMARY

The activities described above have been dedicated to defining the spectral and spatial characteristics of clouds and surface conditions in the polar regions, and to the creation of calibrated, geometrically-correct data sets suitable for quantitative analysis. In addition, some of these activities have begun to explore ways in which this information can be applied to cloud classifications as new methods or as extensions to existing classification schemes. A broad approach has been taken to this information-gathering process since relatively few observational data are available on polar cloud characteristics. A methodology has been developed that uses automated techniques to merge AVHRR and SMMR data, and to apply first-order calibration and zenith angle corrections to the AVHRR imagery. Cloud cover and surface types have been manually interpreted, and manual methods have been used to define relatively pure training areas to describe the textural and multispectral characteristics of clouds over several surface conditions. The effects of viewing angle and bi-directional reflectance differences have been studied for several classes, and the effectiveness of some key components of existing classification schemes (e.g. unsupervised clustering, thresholds, and spatial coherence) has been tested. As additional images are processed, these analyses will be expanded to encompass a larger sample of polar clouds and surfaces.

## 6. PLANNED ACTIVITIES THE NEXT HALF-YEAR

The second half of this project will focus on only those spectral and spatial characteristics that seem most suitable for cloud classification in the polar regions, and will seek ways of incorporating these characteristics into a cloud classifier. Additional images will be analyzed to expand the sample size from which cloud properties are defined. Based on these observed characteristics, the likely sources of error to be expected from cloud classification methods such as spatial coherence, split-window, and bispectral threshold methods will be assessed.

In addition to these tasks, work will begin to investigate correlations between numerical modelling results and observed polar cloud. Spatial and temporal patterns of polar cloudiness predicted using the GISS global climate model will be studied to assess the relative contribution of local versus large-scale processes on polar cloudiness. A second approach will consider methods of comparing observed atmospheric conditions with modelled atmospheres. In particular, the capabilities of the ATRAD radiative transfer model (Wiscombe et al., 1984) will be reviewed. A possible analysis scheme to be considered will compare cloud conditions and surface and cloud temperatures observed in the AVHRR and passive microwave data with the radiative fluxes and atmospheric conditions predicted by the ATRAD model using a "best fit" with observed conditions.

## REFERENCES

- Barry, R.G., Crane, R.G., Schweiger, A. and Newell J. 1987. "Arctic cloudiness in spring from satellite imagery," J. of Climatology, 7, 423-451.
- Bezdek, J.C., 1975. "Mathematical models for systematics and taxonomy," in Proc. Eighth Int. Conf. on Numerical Taxonomy, G. Estabrook (ed.), Freeman, San Francisco, 143-164.
- Cavalieri, D.J., Gloersen, P. and Campbell, W.J., 1984. "Determination of sea ice parameters with the Nimbus 7 SMMR," J. Geophys. Res., 89, 10, 5355-5369
- Coakley, J.A., Jr., 1983. "Properties of multi-layered cloud systems from satellite imagery," J. Geophys. Res., 88, 10, 818-10,828.
- Coakley, J.A., Jr., and D.G. Baldwin, 1984. "Towards the objective analysis of clouds from satellite imagery data," J. Clim. Appl. Meteorol., 23, 1065-1099.
- Coakley, J.A., and F.P. Bretherton, 1982. "Cloud cover from high-resolution scanner data: detecting and allowing for partially filled fields of view," J. Geophys. Res., 87, no. C7, 4917-4932.
- Ebert, Elizabeth, 1987. "A pattern recognition technique for distinguishing surface and cloud types in the polar regions," J. Clim. Appl. Meteor.
- Gerstl, S.A.W. and C. Simmer, 1985. "Radiation physics and modelling for off-nadir satellite sensing of non-Lambertian surfaces." LA-UR-85-4204, Los Alamos National Laboratory.
- Haralick, R.M., and K.S. Shanmugan, 1974. "Combined spectral and spatial processing of Landsat data," Remote Sensing of Environ., 3, 3-13.
- Haralick, R.M., K. Shanmugam, and I. Dinstein, 1973. "Textual features for image classification," IEEE Trans. Syst., Man, Cybern., SMC-3, 610-621.
- Lauritson, L., G.G. Nelson, and R.W. Port, 1979. "Data extraction and calibration of TIROS-N/NOAA A-G radiometer," NOAA Tech. Memor., NESS 107, Natl. Oceanic and Atmos. Admin., Boulder.
- McGuffie, K., R.G. Barry, J. Newell, A. Schweiger, and D. Robinson, 1987. "Intercomparison of satellite-derived cloud analysis for the Arctic Ocean in spring and summer. International Journal of Remote Sensing, in press.

NOAA, 1984. NOAA polar orbiter data user's guide. U.S. Department of Commerce, National Oceanic and Atmospheric Administration, NESDIS, February, 1984.

Parikh, J.A., 1977. "A comparative study of cloud classification techniques," Remote Sens. Environ., 6, 67-81.

Raschke, E., 1987a. "Report of the ISCCP workshop on cloud algorithms in the polar regions," National Institute for Polar Research, WCP-131, WMO/TD-No. 170, Tokyo, Japan, 19-21 August 1986.

Robinson, D.A., Kukla, G.J. and Serreze, M., 1986. "Arctic summer cloudiness," Proc. Sixth Conference on Atmospheric Radiation (Williamsburg, VA), Am. Met. Soc., Boston, MA

Rossow, W.B., 1987. "Application of ISCCP cloud algorithm to satellite observations of the polar regions," in Raschke, E., 1987. "Report of the ISCCP workshop on cloud algorithms in the polar regions," National Institute for Polar Research, WCP-131, WMO/TD-No. 170, Tokyo, Japan, 19-21 August 1986.

Rossow, W.B., F. Mosher, E. Kinsella, A. Arking, M. Desbois, E. Harrison, P. Minnis, E. Ruprecht, G. Seze, C. Simmer, and E. Smith, 1985. "ISCCP cloud algorithm intercomparison," J. Clim. Appl. Meteor., 24, 877-903.

Ruspini, E.H., 1969. "A new approach to clustering," Inf. Control, 15, 22-32.

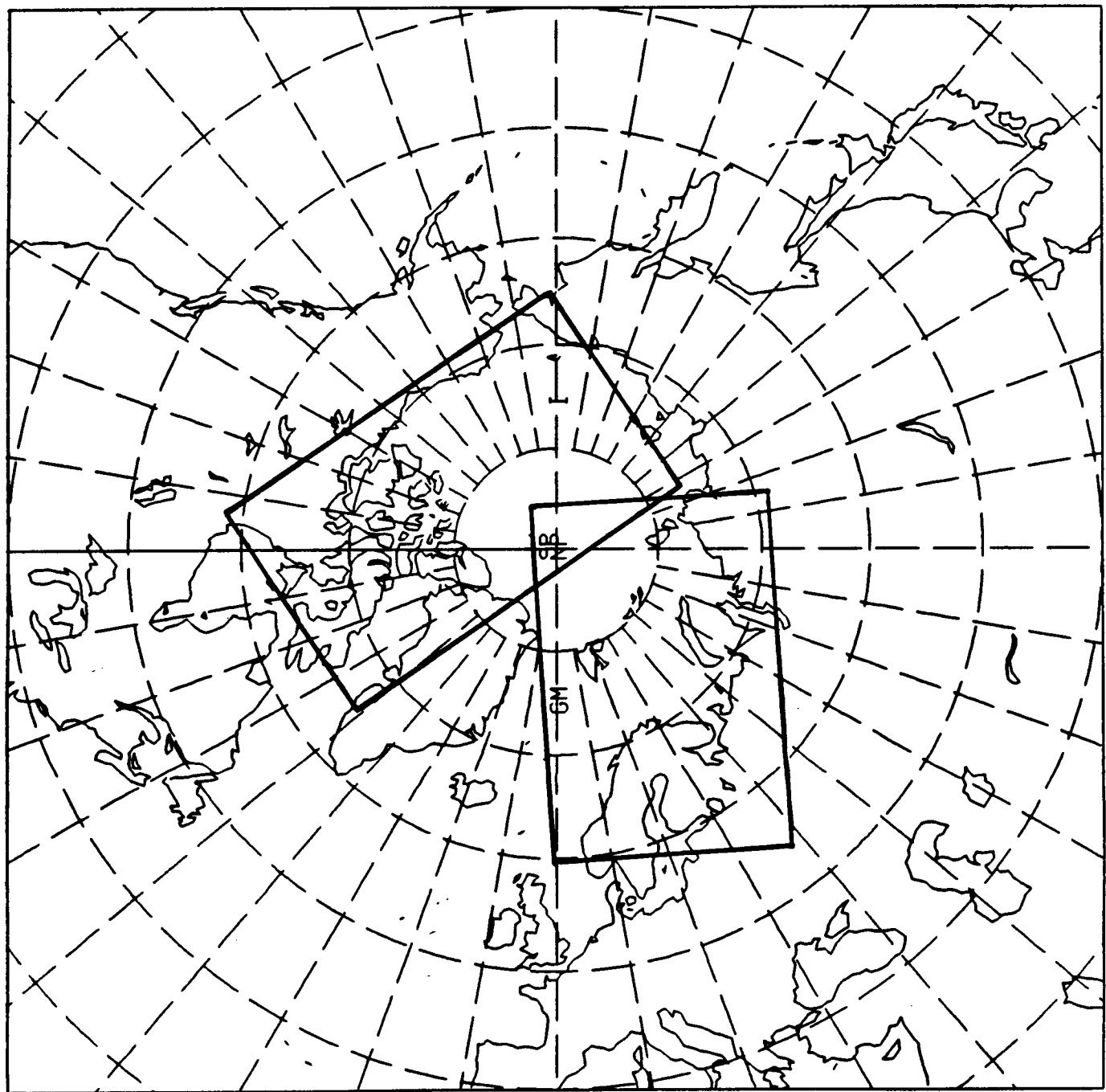
Steffen, K., 1987. "Bidirectional reflectance of snow at 500-600 nm," Large Scale Effects of Seasonal Snow Cover, IAHS Publ. no 166, Vancouver Symposium Proceedings, Aug. 1987, 415-425.

Wiscombe, W.J., R.M. Welch, and W.D. Hall, 1984. "The effect of very large drops on cloud absorption, Part I: Parcel Models. J. Atmos. Sci., 41, 1336-1355.

Wu, R., J.A. Weinman and R.T. Chin, 1985. "Determination of rainfall rates from GOES satellite images by a pattern recognition technique," J. Atmos. Ocean. Tech., 2, 314-330.

## FIGURES

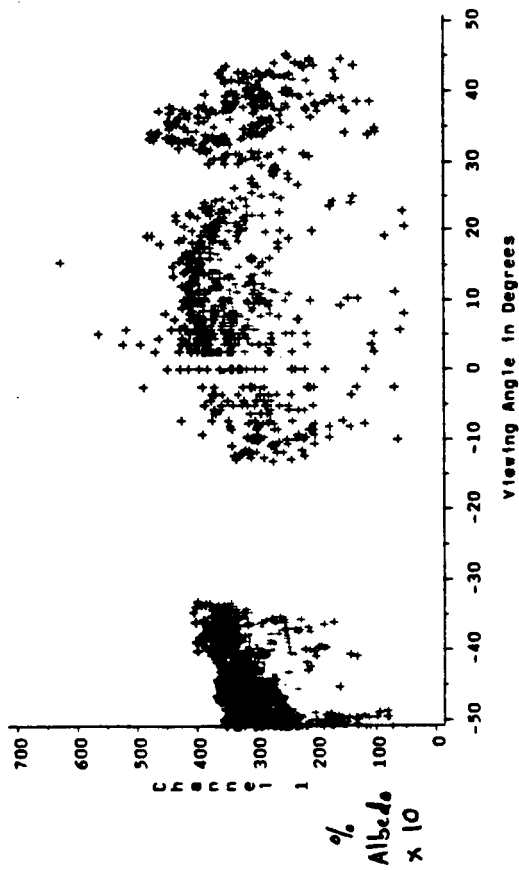
- Figure 1: Areas of coverage of analyses to date.
- Figure 2: Effect of AVHRR viewing angle on channel 1 reflectances and channel 5 temperatures for sea ice and low cloud.
- Figure 3: Representative spectral signatures for interpreted cloud and surface classes in SMMR 18 GHz vertically polarized brightness temperatures, channel 1 reflectances (corrected for zenith angle effects), and Channel 5 thermal temperatures.
- Figure 4: Multispectral cluster plots showing locations of mean + 2 standard deviation class boundaries for surface and cloud classes.
- Figure 5: Multispectral plot of SMMR 18 GHz V. Pol. brightness temperatures, channel 5 thermal temperatures, and channel 1 reflectances.
- Figure 6: SMMR-derived ice concentration and channel 1 reflectances along 2 transects through a portion of a merged AVHRR/SMMR image.
- Figure 7: Simple texture representations for sea ice and low cloud in channels 1 and 4.
- Figure 8: Spatial coherence plot containing a typical mix of polar clouds and surfaces.
- Figure 9: Spatial coherences of individual cloud and surface classes.



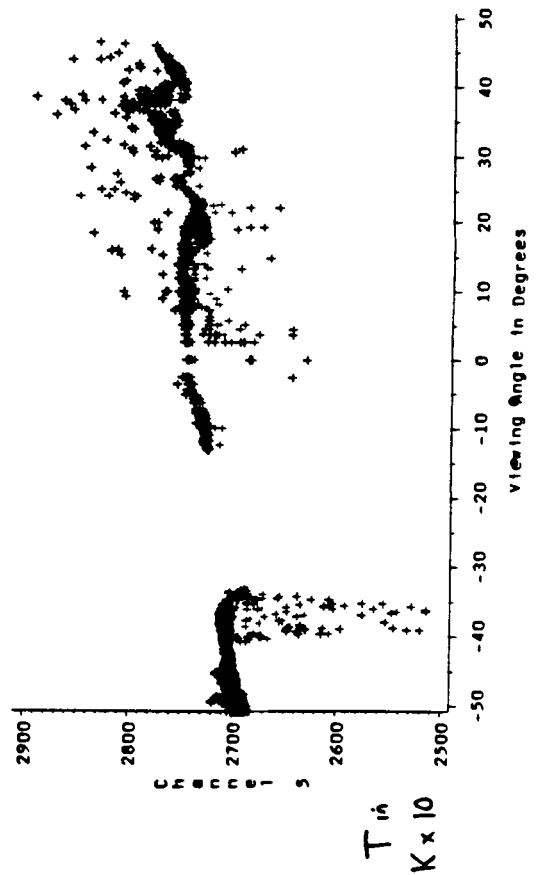
SUPHAP 0. 90.0. 90.0. 0.0. 50.0. 50.0. 50.0. 50.0. 4. 10. 0. 01

FIG. 1

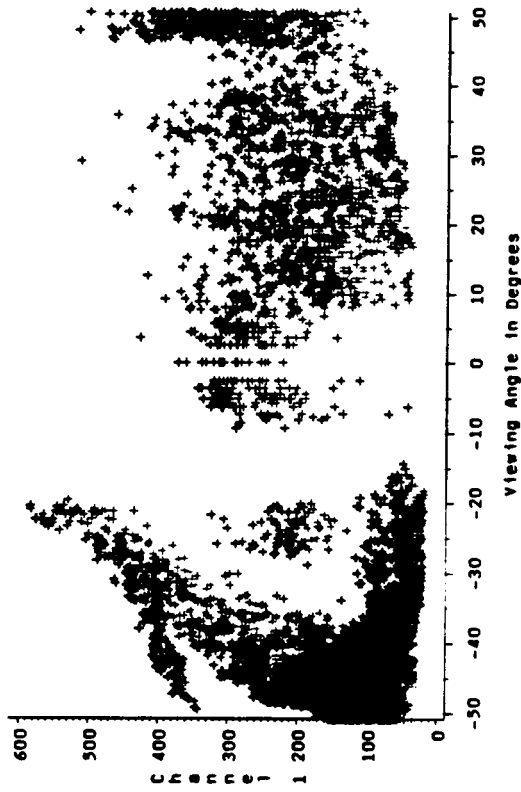
AVHRR CH01 BY VIEWING ANGLE  
CLASS=SEA ICE



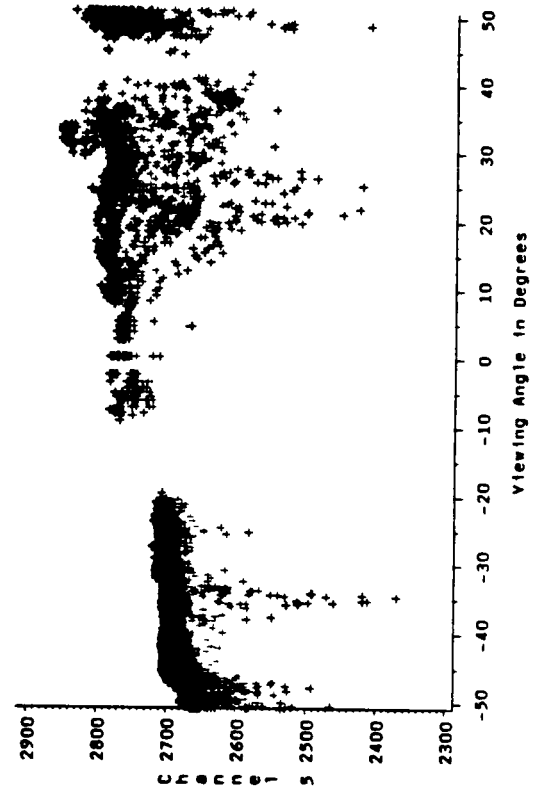
AVHRR CH05 BY VIEWING ANGLE  
CLASS=SEA ICE



AVHRR CH01 BY VIEWING ANGLE  
CLASS=LOW CLOUD



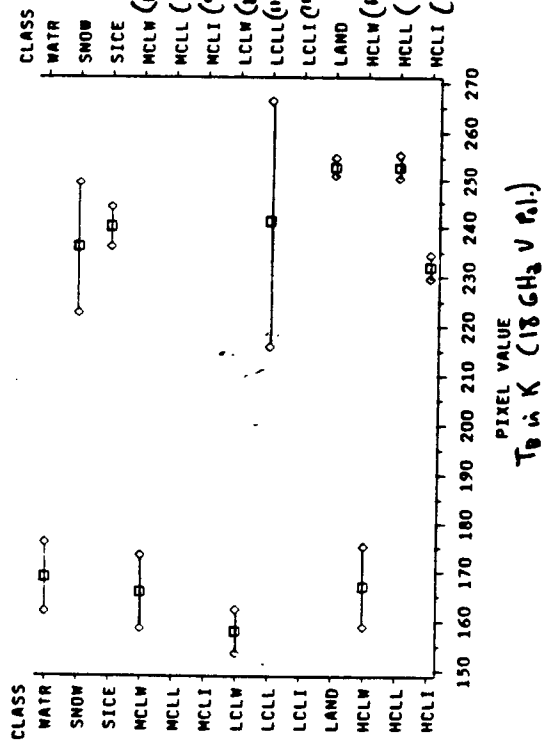
AVHRR CH05 BY VIEWING ANGLE  
CLASS=LOW CLOUD



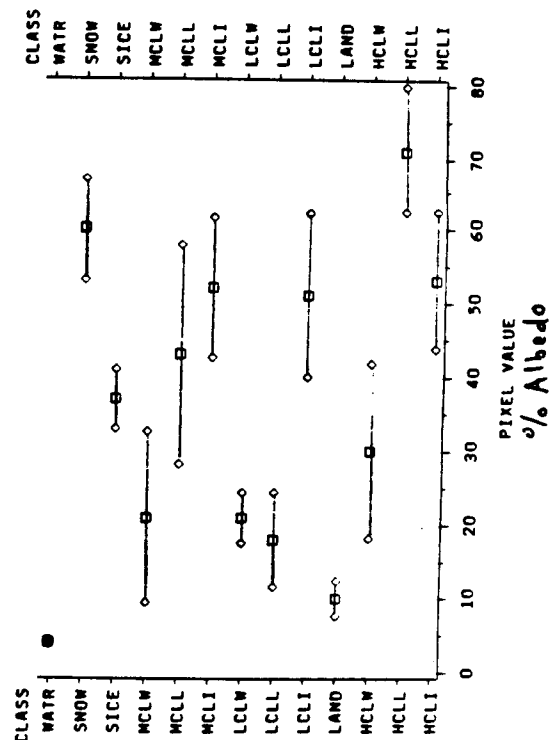
ORIGINAL PAGE IS  
OF POOR QUALITY

FIG. 2

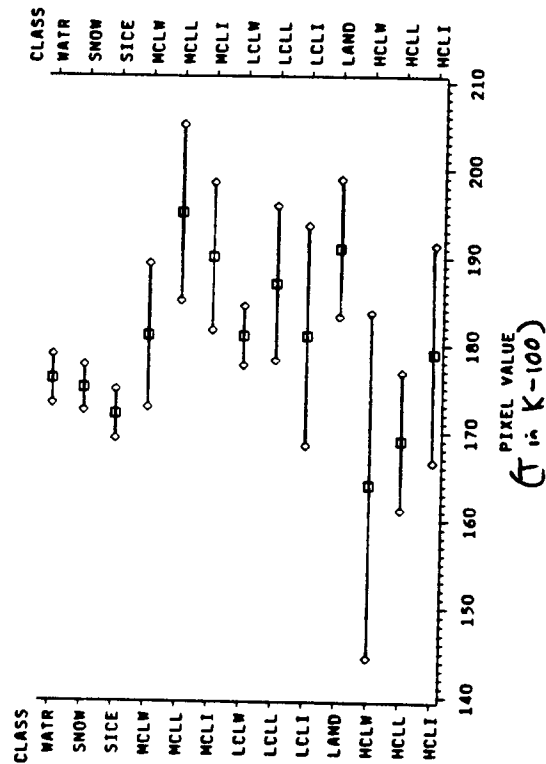
GBT PIXEL VALUES BY CLASS  
Mean  $\pm$  2 Standard Deviations  
FEATURE=18V1



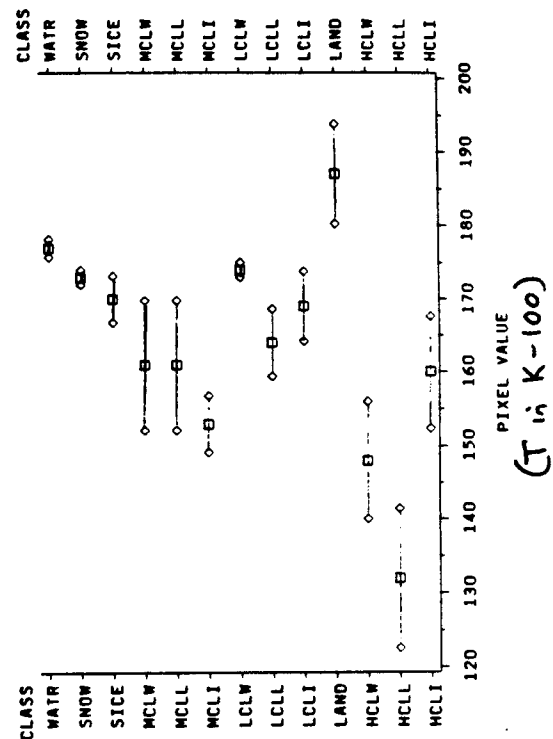
GBT PIXEL VALUES BY CLASS  
Mean  $\pm$  2 Standard Deviations  
FEATURE=CH01



GBT PIXEL VALUES BY CLASS  
Mean  $\pm$  2 Standard Deviations  
FEATURE=CHT3



GBT PIXEL VALUES BY CLASS  
Mean  $\pm$  2 Standard Deviations  
FEATURE=CHT5

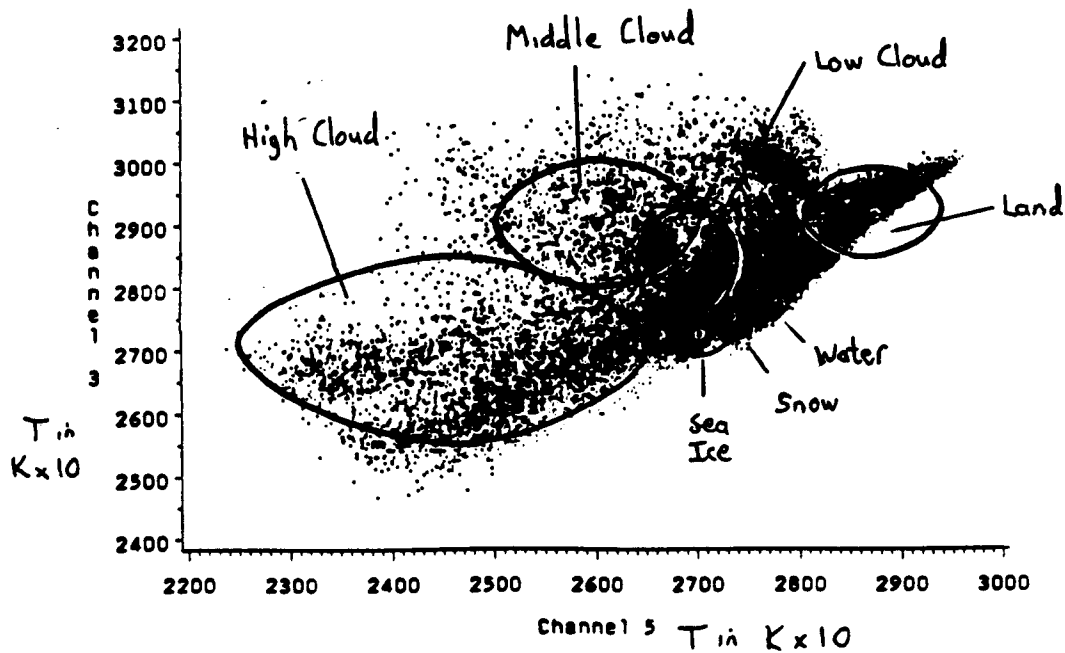
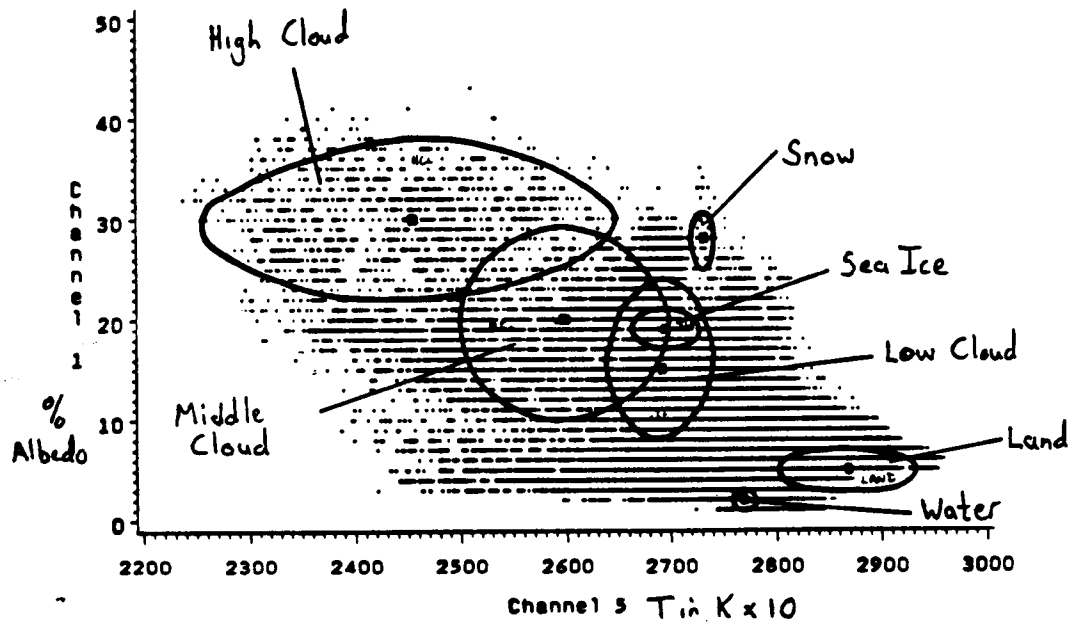
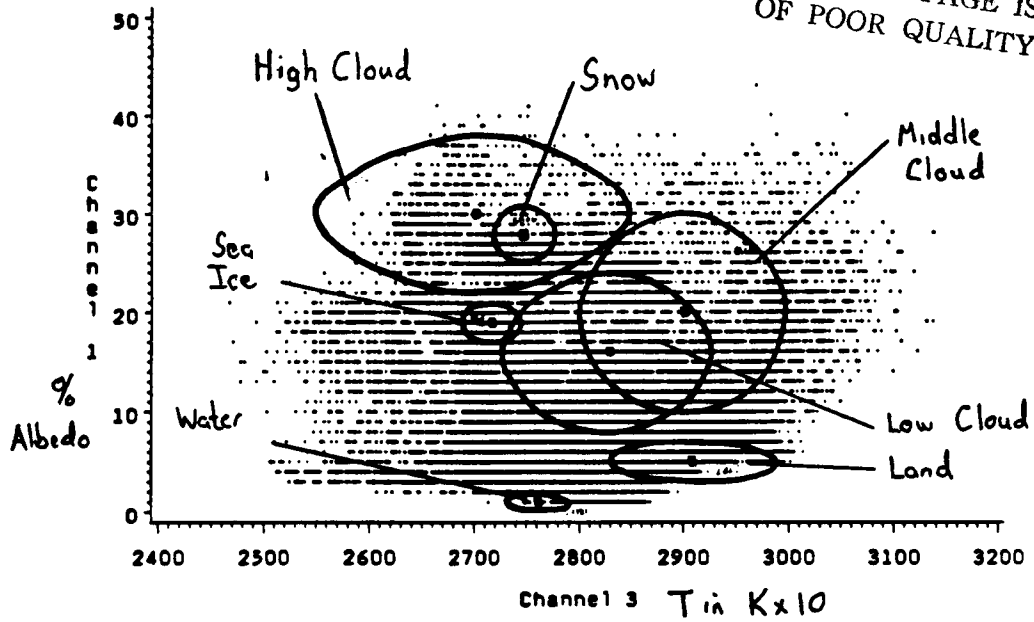


ORIGINAL PAGE IS  
OF POOR QUALITY

FIG. 3

FIG. 4

ORIGINAL PAGE IS  
OF POOR QUALITY



# MIDDLE CLOUD OVER LAND AND OVER WATER AVHRR and SMNR

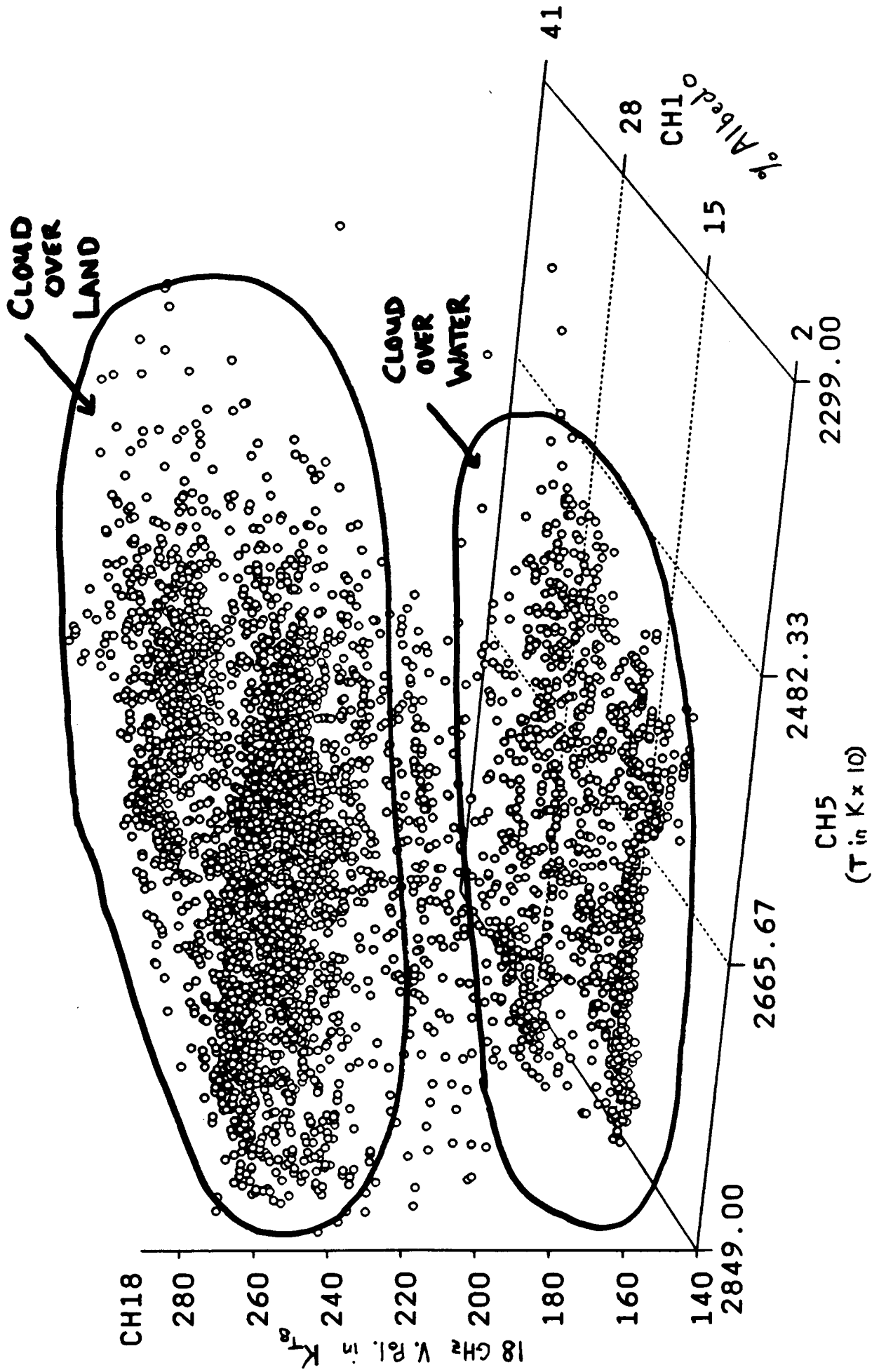


FIG. 5

merged avhrr and smmr, 2 JULY 1984

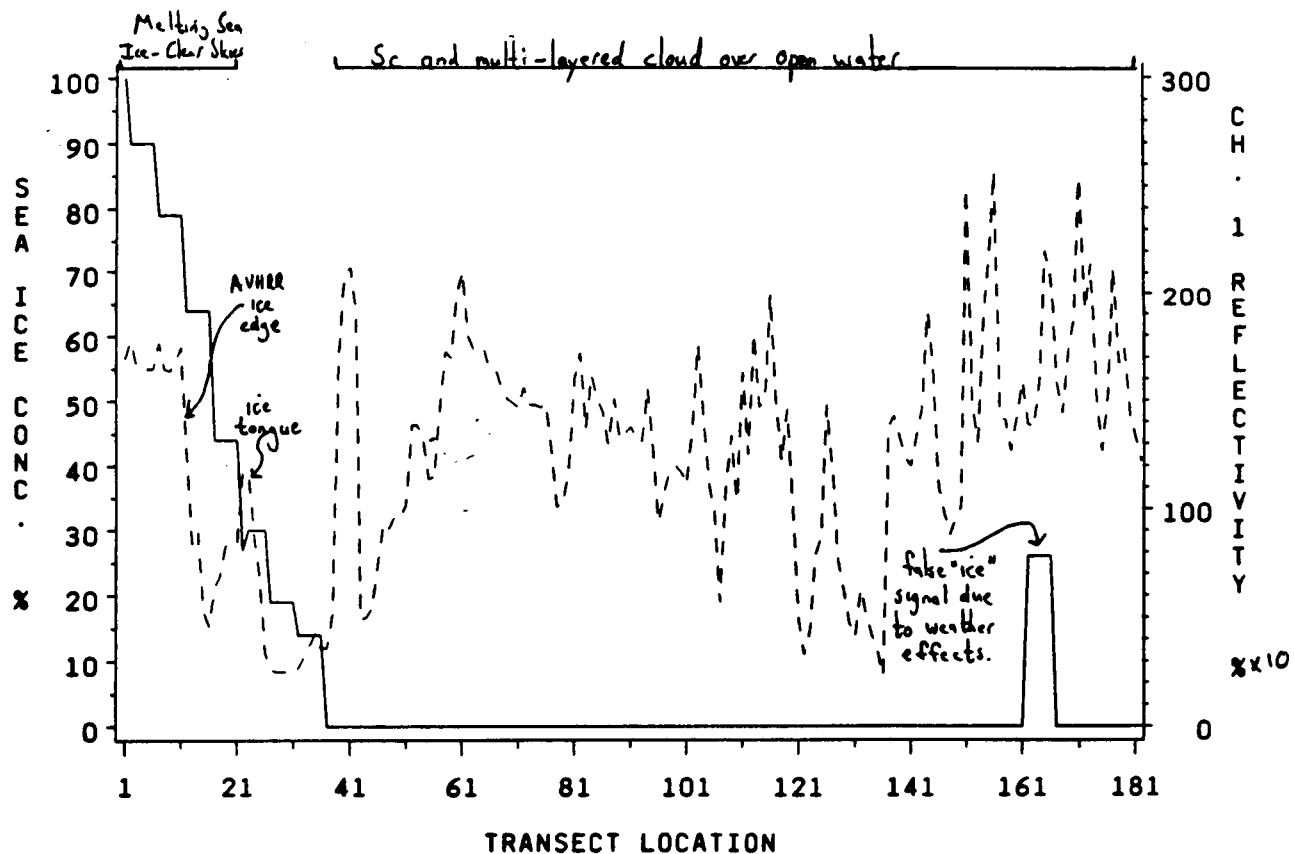
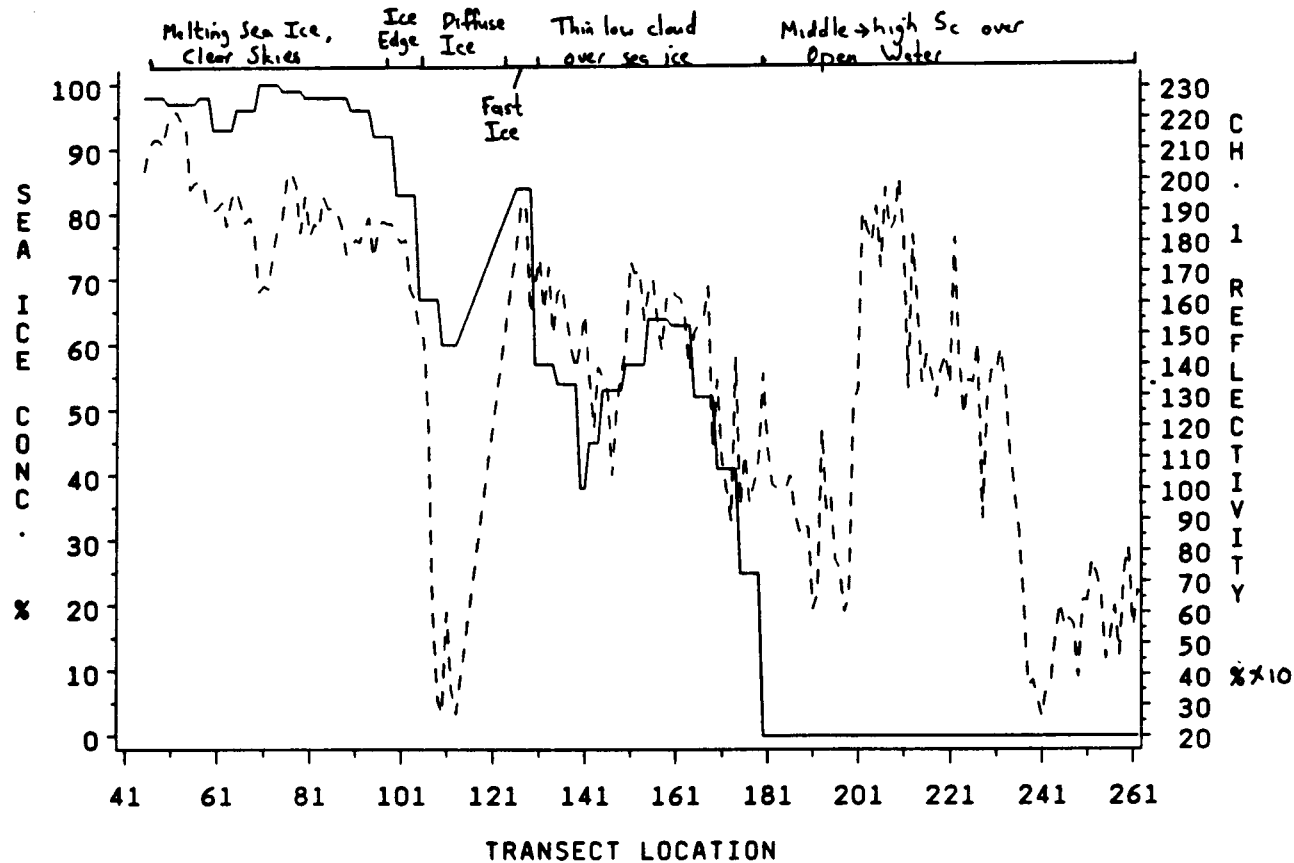
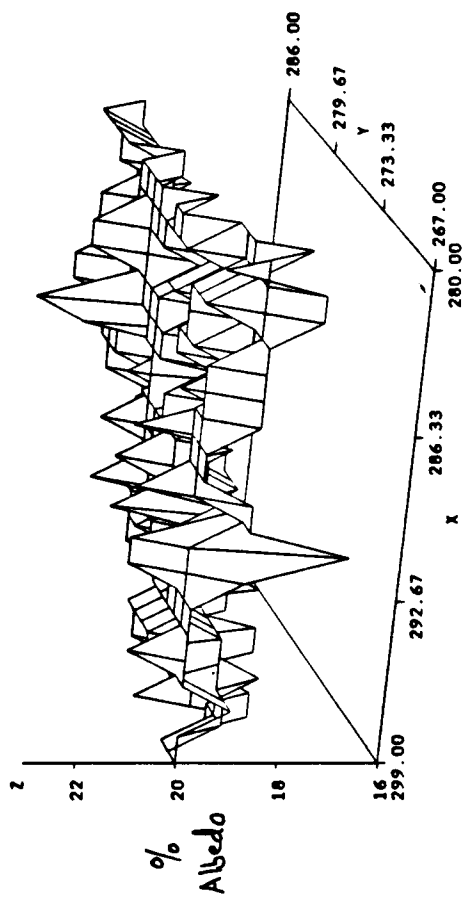


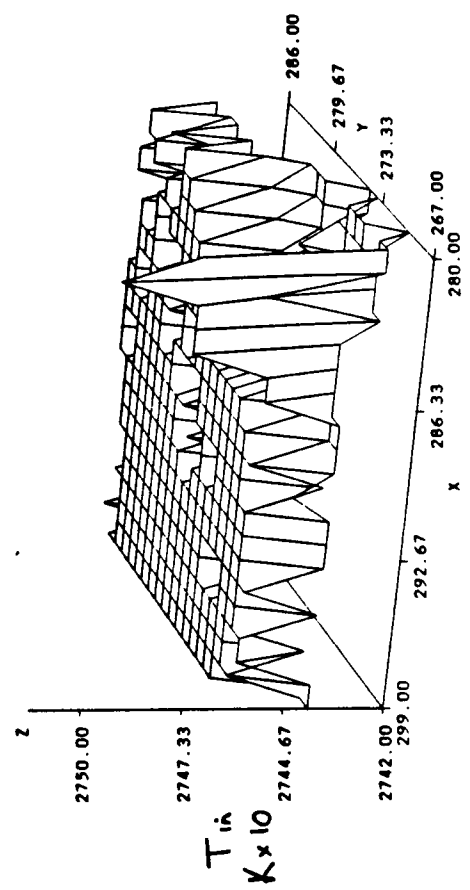
FIG. 6

ORIGINAL PAGE IS  
OF POOR QUALITY

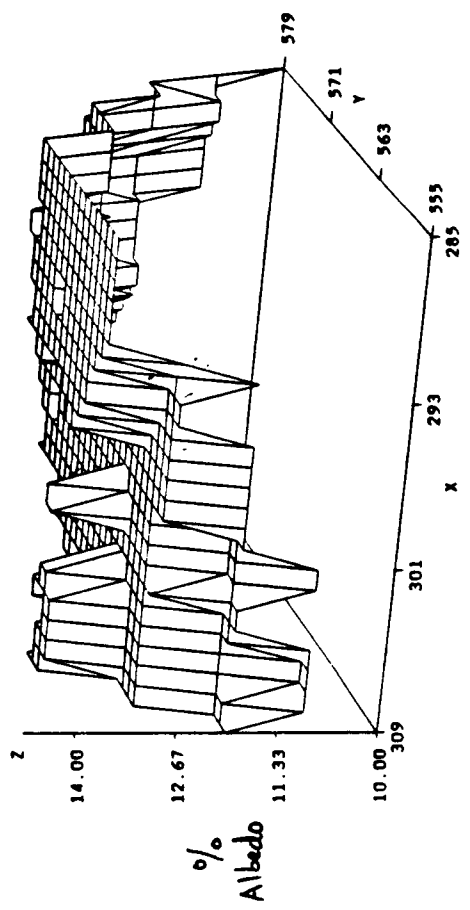
TEXTURE: SEA ICE MEDIUM CONCENTRATION  
AVER CMT1



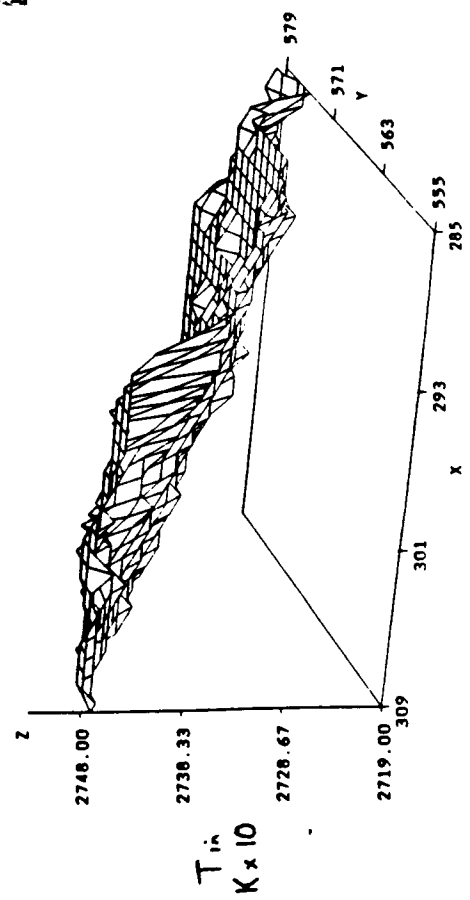
TEXTURE: SEA ICE MEDIUM CONCENTRATION  
AVER CMT4



TEXTURE: LOW CLOUD OVER WATER  
AVER CMT1



TEXTURE: LOW CLOUD OVER WATER  
AVER CMT4



ORIGINAL PAGE IS  
OF POOR QUALITY

FIG. 7

# STANDARD DEVIATION BY MEAN: 8X8 CELL, GB1CHT4

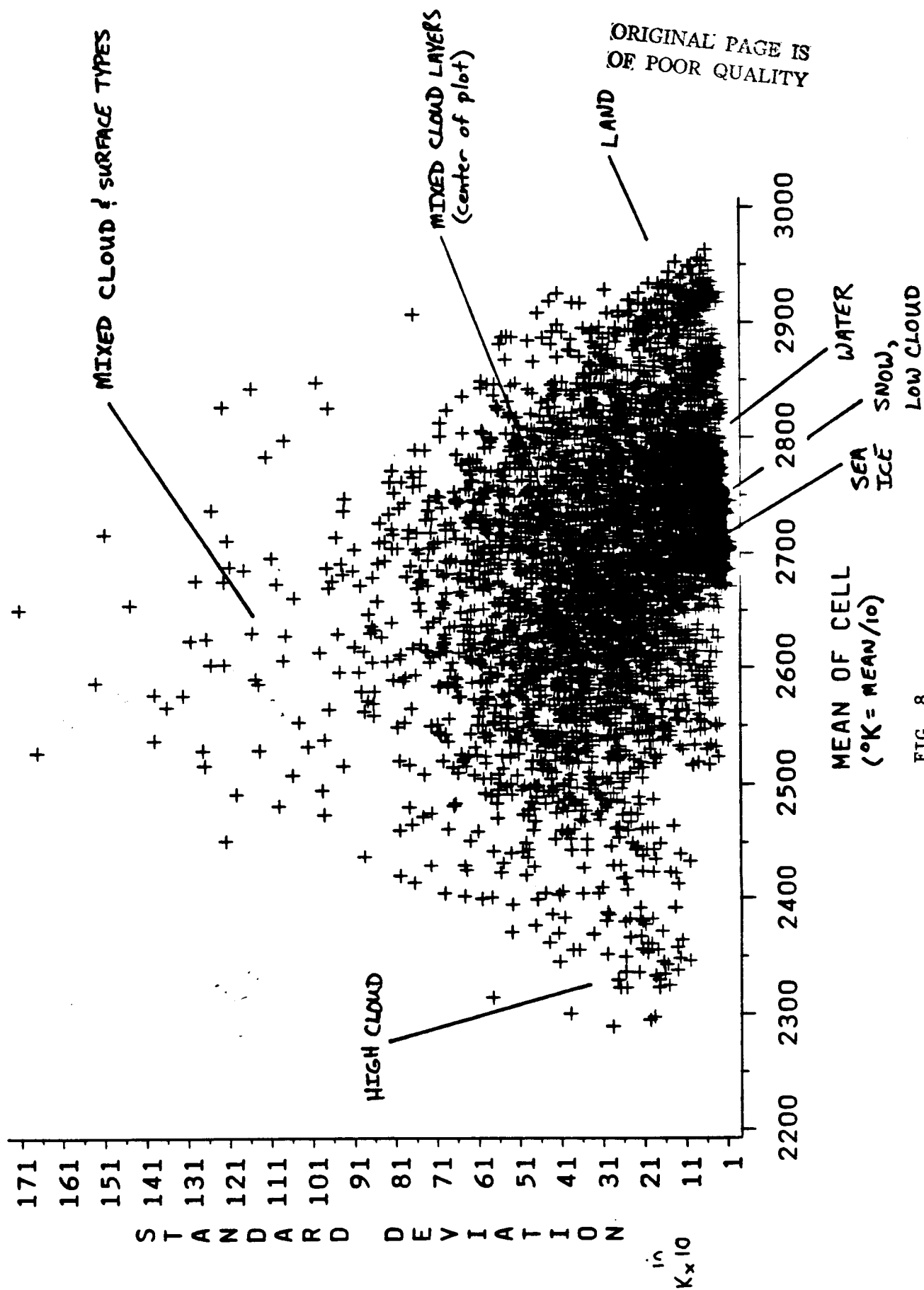
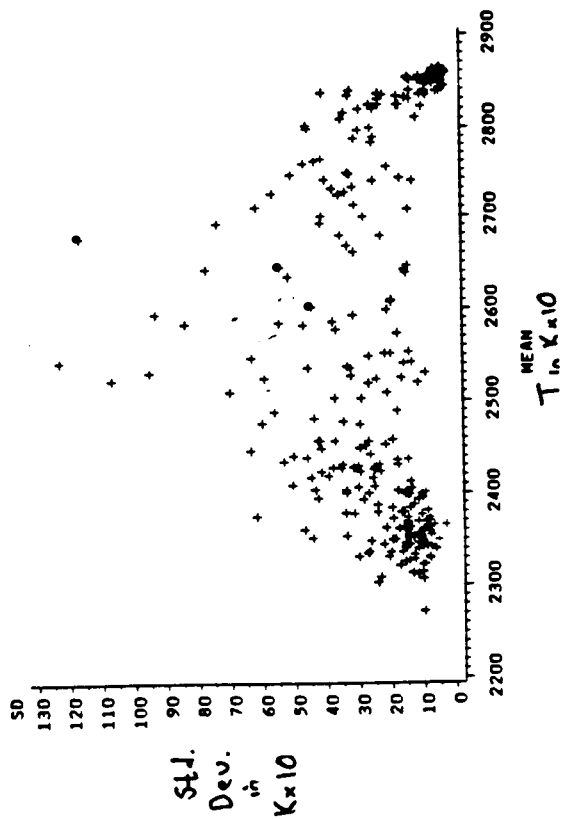
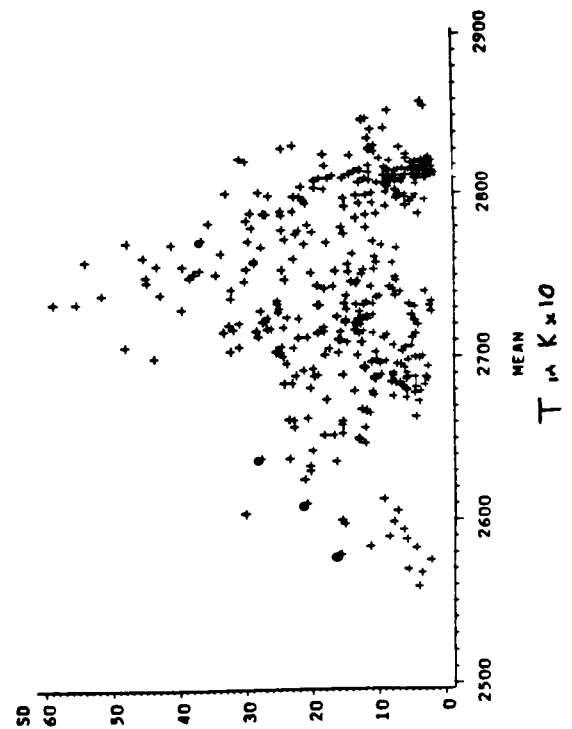


FIG. 8

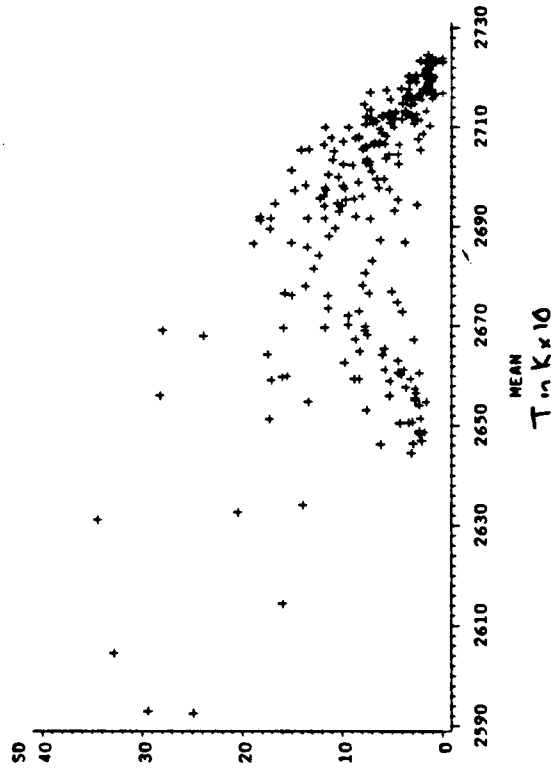
MEANS VS. STANDARD DEVIATION, 4 X 4 CELLS  
GBT HIGH CLOUD OVER LAND



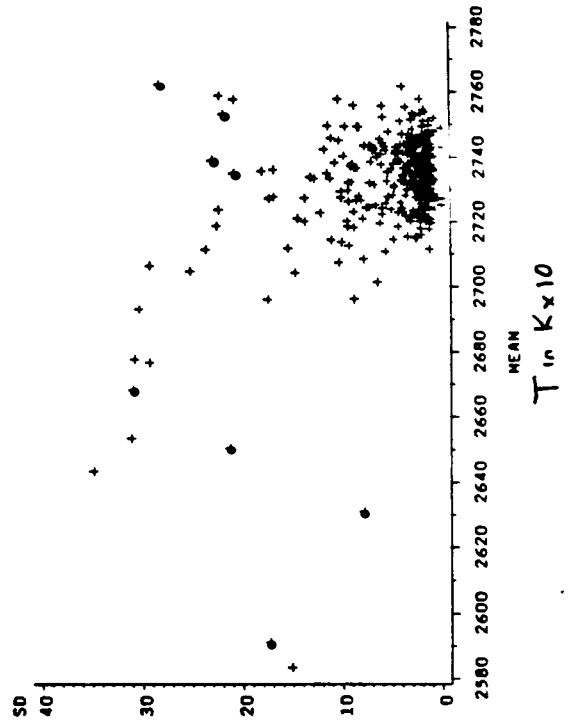
MEANS VS. STANDARD DEVIATION, 4 X 4 CELLS  
GBT & GLT MIDDLE CLOUD OVER LAND



MEANS VS. STANDARD DEVIATION, 4 X 4 CELLS  
GLT MIDDLE CLOUD OVER ICE



MEANS VS. STANDARD DEVIATION, 4 X 4 CELLS  
GBT & GLT LOW CLOUD OVER WATER



ORIGINAL PAGE IS  
OF POOR QUALITY.

FIG. 9